Int. J. Multiphase Flow Vol. 18, No. 6, pp. 803–820, 1992
Printed in Great Britain

0301-9322/92 $5.00 + 0.00
Pergamon Press Ltd

USE OF LAGRANGIAN METHODS TO DESCRIBE DROP DEPOSITION AND DISTRIBUTION IN HORIZONTAL GAS–LIQUID ANNULAR FLOWS

J. L. BINDER and T. J. HANRATTY
Departments of Chemical and Nuclear Engineering, University of Illinois, Urbana, IL 61801, U.S.A.

(Received 15 November 1990; in revised form 28 July 1992)

Abstract—Drop distribution and deposition in horizontal gas–liquid annular flow is described by a diffusion model, which views the concentration field as the result of dispersion from a distribution of sources. Drops originating from a wall source are considered to diffuse in a field of homogeneous turbulence, while simultaneously being swept downward by the gravitational field. Deposition is assumed to be controlled by two mechanisms operating in parallel, and boundary conditions are derived which correctly satisfy conservation of mass. This analysis for an instantaneous source is shown to be equivalent to considering diffusion in a coordinate system moving with the settling velocity of the particles. The results are found to be useful for understanding droplet distribution and deposition.

Key Words: annular flow, stratification, horizontal flows, deposition rates, droplet profiles, Lagrangian methods

1. INTRODUCTION

For gas–liquid flow in enclosed ducts an annular pattern exists at high gas velocities. Part of the liquid moves along the wall as a liquid layer and part as droplets entrained in the gas. There is an exchange of liquid between the liquid layer and the core characterized by the rate of atomization per unit area, R_A, and the rate of deposition per unit area, R.

For annular flows in a horizontal pipe the influence of the gravitational field causes a stratification of the drops in the gas and an asymmetric distribution of the liquid flowing along the wall. This paper is concerned with determining flow parameters which control the degree of stratification and the spatial variation of the rate of deposition.

The system considered is a two-dimensional rectangular channel, because of its simplicity compared to a circular pipe. Liquid of uniform height is considered to be flowing along the top and bottom walls. Because of gravitational effects, droplet concentrations, the rate of atomization and the height of the liquid layer are larger on the bottom wall.

Research on this system is limited to the laboratory studies by Namie & Ueda (1972) and McCoy & Hanratty (1975). Namie & Ueda used a diffusion model to describe droplet transfer but did not include the effects of gravitational settling. Anderson & Russell (1970) and James *et al.* (1980) produced models that are based on the analysis of deterministic trajectories of the droplets. McCoy & Hanratty (1975) argued that deposition is controlled by gravitational settling at low gas velocities. The calculations presented in this paper incorporate these ideas of previous researchers but use a different theoretical framework.

The Lagrangian analysis of particle diffusion recently presented by Binder & Hanratty (1991) for vertical gas–liquid annular flows is extended by including the effects of gravitational settling. The calculations are restricted to drops that have stopping distances larger than the viscous wall layer. Non-homogeneities in the turbulence close to the wall are, therefore, ignored and the problem is simplified by assuming a uniform velocity.

The concentration field is pictured as resulting from a distribution of sources. The central problem is, then, to describe the behavior of one instantaneous source of drops whose magnitude is specified. Because of limited understanding of the entrainment process it is assumed that the turbulence properties of the drops entering the field are proportional to the turbulence properties of the fully entrained droplets, and that the droplets have the same streamwise velocity as the gas. The influence of turbulence on the spread of particles downstream of the source is described by

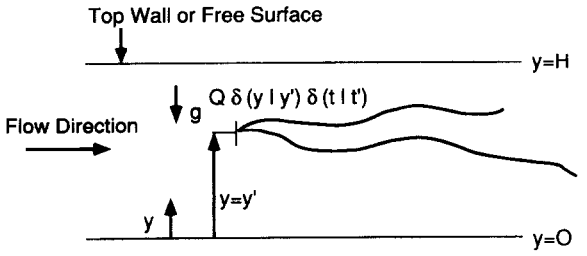

Figure 1. Idealized picture of line-source diffusion.

a diffusion equation with a diffusion coefficient that varies with time. A method for describing the boundary conditions at the surfaces developed by Lee *et al.* (1989) is used. The influence of the gravitational field on the drop motion is assumed to be independent of the turbulence. It causes an average deterministic velocity, V_y, in a direction perpendicular to the wall. This velocity is a function of the amount of time particles from a source have been in the field and reaches a free-fall value only after a sufficiently long time.

Deposition is considered to occur by turbulence and gravitational settling acting in parallel. The flux of drops to a wall due to turbulence is described as a free flight from a position beyond the outer edge of the viscous wall layer to the wall, defined as vC_S, where C_S is the concentration at the wall. Velocity v, is represented as the product of the magnitude of the normal velocity fluctuations of the drops and the fraction, f, of the particles at the outer edge of the viscous wall layer that are caused to move toward the wall by turbulence:

$$v = \sqrt{\frac{2}{\pi}} f(\overline{v_y^2})^{1/2}. \qquad [1]$$

The turbulence is pictured to bring the drops to their free-flight location by turbulent diffusion so that at the wall

$$-\varepsilon_P \frac{\partial C}{\partial y} = vC_S. \qquad [2]$$

2. FORMULATION OF THE DIFFUSION EQUATION FOR A POINT SOURCE

The situation considered is shown in figure 1. An instantaneous line source of drops enters the field at $y = y'$ and at time $t = t'$. Typically the source will be located at the lower ($y' = 0$) or upper boundary ($y' = H$); however, in some situations the sources could be located elsewhere. The drops emitted by an instantaneous source are entrained into the flow and eventually deposit out. Deposition at the top boundary will be due to turbulent diffusion; deposition on the lower boundary will be due to a combination of diffusion and gravitational settling.

Following arguments presented in previous papers (Binder & Hanratty 1991; Hanratty 1956, 1958; Hanratty & Flint 1958; Eckleman & Hanratty 1972), the time-dependent equation describing turbulent diffusion from an instantaneous source in a homogeneous field is given by

$$\frac{\partial C(y,t)}{\partial t} + V_y(t-t')\frac{\partial C(y,t)}{\partial y} = \varepsilon_P(t-t')\frac{\partial^2 C(y,t)}{\partial y^2} + Q\delta(y \mid y')\delta(t \mid t'), \qquad [3]$$

where Q is the source strength, with units of mass per unit area, and δ is the Dirac delta function. Since variations in the velocity profile are ignored, time can be converted to distance downstream with the transformation $dx = V_x t$, where V_x is the mean velocity of the particles in the x-direction.

The particle diffusivity is characterized by the mean-square of the turbulent velocity fluctuations, $(\overline{v_y^2})$ and a Lagrangian time scale, τ_P. As shown in Taylor's (1921) analysis of diffusion from an infinitesimal source, the diffusivity is a function of the dispersion time or the time the drop has been in the flow field. For small times the diffusivity increases linearly; as time increases it

approaches an asymptotic limit. This behavior is represented by the following equation, which assumes the Lagrangian correlation is given by an exponential function (Hanratty & Flint 1958):

$$\varepsilon_P(t-t') = \overline{v_y^2}\tau_P\left\{1-\exp\left[-\frac{(t-t')}{\tau_P}\right]\right\}. \quad [4]$$

The time-dependent velocity, V_i, is obtained by solving the equation of motion of the particle to obtain an average trajectory. The only forces considered are those due to gravity and particle drag, and it is assumed that the turbulence does not, on average, affect the drag coefficient. The equation for V_i is, therefore, given as

$$\frac{dV_i}{dt} = -\frac{3}{4}\frac{\rho_f}{\rho_P}\frac{c_D}{d_P}|\mathbf{V}-\mathbf{U}|\,V_i - g\left(1-\frac{\rho_f}{\rho_P}\right), \quad [5]$$

with

$$V_i(t=t') = V_i'. \quad [6]$$

For small particle Reynolds numbers ($Re_P < 1$),

$$c_D = \frac{24}{Re_P}; \quad [7]$$

and for intermediate particle Reynolds numbers ($1 < Re_P < 1000$),

$$c_D = \frac{18.5}{Re_P^{3/5}}, \quad [8]$$

where Re_P is based on $|\mathbf{V}-\mathbf{U}|$.

Not enough information is available about the manner in which the droplets enter the gas flow. For simplicity it is assumed that they are initially entrained in the turbulence with a velocity proportional to the intensity of the turbulent velocity fluctuations, so that $V_y' = \sqrt{2/\pi}\,(\overline{v_y^2})^{1/2}$. A reasonable assumption for the initial x-component of the velocity is $V_x' = S'U_x$, where U_x is the bulk velocity of the fluid. For simplicity the initial slip ratio, S', is taken as unity; however, it would be of interest to explore other values.

The ability of the particle to respond to the fluid turbulence is represented by the reciprocal time constant, β, defined as

$$\beta = \frac{3c_D\rho_f}{4d_P\rho_P}|\mathbf{V}-\mathbf{U}|. \quad [9]$$

For the Stokes flow regime,

$$\beta = \frac{18\mu_f}{d_P^2\rho_P}, \quad [10]$$

where μ_f is the dynamic viscosity of the fluid, ρ is the density and d is diameter. This analysis is restricted to situations where the diffusion length scale characterizing particle motion, $(\overline{v_y^2})^{1/2}\,\tau_P$, is less than the channel height and larger than the viscous wall region. McCoy & Hanratty (1975) pointed out that this latter restriction is satisfied if $1/\beta^+ = (u_*^2/\upsilon_f\beta) > 20$; υ_f is the kinematic viscosity of the fluid. The consequence of neglecting effects associated with non-homogeneities of the velocity field in [3] and [5] has not been evaluated.

3. FORMULATION OF THE BOUNDARY CONDITIONS

From [1] and [2] and the discussion presented by Lee *et al.* (1989), the following boundary conditions are used to solve [3] for the behavior of a line source at the bottom wall:

$$\varepsilon_P(t-t')\frac{\partial C(y=0,t)}{\partial y} = f(t-t')\sqrt{\frac{2}{\pi}}\,(\overline{v_y^2})^{1/2}C(y=0,t) \quad [11]$$

at the lower boundary, $y=0$, at time t; and

$$-\varepsilon_P(t-t')\frac{\partial C(y=H,t)}{\partial y} = f(t-t')\sqrt{\frac{2}{\pi}}\,(\overline{v_y^2})^{1/2}C(y=H,t) \quad [12]$$

at the upper boundary, $y = H$, at time t. The fraction of the drops moving towards the bottom wall is assumed to have the form

$$f(t-t') = \frac{1}{2}\left[1 - \exp\left(-\frac{t-t'}{\tau_P}\right)\right], \quad [13]$$

where τ_P is the Lagrangian time scale. It is to be noted that [11] and [12] represent an equality between turbulent diffusion and free flight to the boundary. The gravitational settling term does not appear in these boundary conditions because it is already included in [3].

The rationale behind this equation is that f is a multiplier of the term representing the magnitude of the turbulent velocity fluctuations that accounts for the previous history of the drops. Drops that have been in the field for a large time are just as likely to have a plus or minus sign, so one-half will be moving toward the wall (in the negative direction). Consequently, one can expect $f = 1/2$ for large $(t - t')$. Drops which are entering the field from the bottom wall are moving in the positive direction, so that $f = 0$ for $(t - t') \to 0$. The function $f(t - t')$ represented by [13], approaches 1/2 asymptotically with the same dependency as the diffusivity, given in [4]. The choice of this function is made for mathematical convenience, although it is physically reasonable since it would be expected that $f(t)$ would not equal 1/2 until the dispersing droplets have obtained the haphazard motion characteristic of diffusion at large times.

The fraction of the drops moving toward the top wall is taken to be 1/2 in [12] because they have been in the field for a long time. Equations similar to [11] and [12] can be used as boundary conditions for line sources at the top wall.

A justification for boundary conditions [11] and [12] is obtained by integrating [3], with respect to time from $t = t'$ to $t = \infty$ and with respect to channel height from $y = 0$ to $y = H$. A mass balance for drops in the flow field resulting from one instantaneous source is obtained:

$$\int_0^\infty dt V_y(t-t')[C(y=H,t) - C(y=0,t)] - \int_0^\infty dt \varepsilon_P(t-t') \times \left[\frac{\partial C(y=H,t)}{\partial y} - \frac{\partial C(y=0,t)}{\partial y}\right] = \int_0^\infty dt \int_0^H dy Q\delta(y \mid y')\delta(t \mid t'). \quad [14]$$

In [14] the condition has been used that the concentration of drops at time $(t - t') = 0$ is zero. In addition, the concentration of drops at large t is zero because all of them have deposited out. The term on the right-hand side of [14] is the total mass emitted by one source. This must be equal to the total amount of mass deposited. For deposition rates of R_0 at $y = 0$ and of R_H at $y = H$ the following equation is obtained:

$$\int_0^\infty dt \int_0^H dy Q\delta(y \mid y')\delta(t \mid t') = \int_0^\infty dt[R_0(t-t') + R_H(t-t')]. \quad [15]$$

The particle flux at a boundary is given as the sum of contributions due to turbulent velocity fluctuations and to gravitational settling:

$$R_i = R_i^T + R_i^S, \quad [16]$$

where

$$R_0^T = vC(y=0,t), \quad [17]$$

$$R_H^T = vC(y=H,t) \quad [18]$$

and v is defined by [1]. The contribution due to settling is

$$R_0^S = V_y(t-t')C(y=0,t) \quad [19]$$

at the bottom wall and

$$R_H^S = V_y(t-t')C(y=H,t) \quad [20]$$

at the top wall. If [15] is substituted into [14] it follows from [16]–[20] that the derivatives appearing in the second term on the left-hand side of [14] need to be defined by [11] and [12] to satisfy

conservation of mass. The term representing a flux of particles to the top wall due to the deterministic velocity V_y, i.e. R_H^S, would usually be negative since particles reaching the top wall would have reached their free-fall velocity and be settling away from the wall. Consequently, R_H can be positive or negative depending on whether $R_H^T + R_H^S$ is greater or less than zero. The physical picture that emerges from this analysis is that a point source of particles is emitted into a field of homogeneous turbulence and begins to diffuse. The spread of the particles is governed by time-dependent turbulent diffusion with a diffusivity given by [4]. A settling velocity imposed by the gravitational field, that serves to sweep the particles downward, operates in parallel.

This interpretation for the boundary conditions and a rationale for [3] evolve in a direct way if the diffusion equation is formulated in a coordinate system moving with the velocity $V_y(t - t')$. The following transformation of the space coordinate y is used:

$$\eta(y, t) = y + \int V_y \, dt. \qquad [21]$$

Equation [3] then takes the same form as the diffusion equation for a field without a gravitational field:

$$\frac{\partial C}{\partial t} = \varepsilon_P(t - t') \frac{\partial^2 C}{\partial \eta^2} + \text{SOURCE}; \qquad [22]$$

and the boundary conditions clearly do not need terms involving the settling velocity if the diffusion and settling processes are assumed independent of one another.

The preceding analysis presents a framework from which to interpret the deposition measured for the horizontal transport of a particulate. Deposition constants (k, k_0, k_H) can be defined as

$$R = kC_B, \qquad [23a]$$

$$R_0 = k_0 C_B \qquad [23b]$$

and

$$R_H = k_H C_B, \qquad [23c]$$

where C_B is the bulk concentration given by

$$C_B = \frac{1}{H} \int_0^H C(y) \, dy. \qquad [24]$$

In many physical situations involving horizontal flows the majority of the transported mass will deposit on the lower boundary. Since turbulent diffusion and gravitational settling are parallel processes, k can be considered to be the sum of deposition constants for turbulence and settling defined as follows:

$$k = k^T + k^s. \qquad [25]$$

4. SCALING RELATIONS FOR ANNULAR FLOW

Following Binder & Hanratty (1991) the problem is made dimensionless in the remainder of the paper by the following scaling:

$$y \to \frac{y}{H}, \; t \to \frac{tu_*}{H}, \; \varepsilon_P \to \frac{\varepsilon_P}{u_* H}, \; (\overline{v_y^2})^{1/2} \to \frac{(\overline{v_y^2})^{1/2}}{u_*}, \; V_y \to \frac{V_y}{u_*}, \; C \to \frac{Cu_*}{R_A}, \qquad [26]$$

where u_* is the friction velocity of the flow. The fluid diffusivity, ε_t, the integral time scale, τ_t, and the turbulence intensity are related to the friction velocity in the following way (Vames & Hanratty 1988):

$$\frac{\varepsilon_f}{u_* H} = 0.037 \qquad [27]$$

$$\frac{\tau_f u_*}{H} = 0.046 \qquad [28]$$

and

$$(\overline{u_y^2})^{1/2} = 0.9u_* \qquad [29]$$

near the boundaries. Thus, the dimensionless drop diffusivity, drop time scale and drop turbulent intensity are proportional to the ratios of the drop values to the fluid values. The dimensionless settling velocity is scaled with the friction velocity.

The dimensionless form of differential equation [3] is then

$$\frac{\partial C(y,t)}{\partial t} + V_y(t-t')\frac{\partial C(y,t)}{\partial y} = \varepsilon_P(t-t')\frac{\partial^2 C(y,t)}{\partial y^2} + \delta(y \mid y')\delta(t \mid t'), \qquad [30]$$

where $\delta(y \mid y')$ and $\delta(t \mid t')$ in [3] have, respectively, been made dimensionless by multiplying by H and by H/u_*. Noting that $\rho_f \ll \rho_P$ for liquid droplets in a gas, the equation describing the deterministic part of the drop motion is written as

$$\frac{dV_y}{dt} = -\gamma V_y^2 - \frac{1}{Fr}, \qquad [31]$$

where

$$\gamma = \frac{3\rho_f H}{4\rho_P d_P} c_D \qquad [32]$$

and the Froude number, Fr, is defined as

$$Fr = \frac{u_*^2}{gH}. \qquad [33]$$

In the context of [5] and [31], Fr represents the relative importance of drag and gravitational forces on the deterministic velocity.

Streamwise slip between the fluid and the drop velocity is assumed to be small compared to the fluid friction velocity. Additionally, the drop settling velocity is assumed equal to or less than the friction velocity. This assumption regarding the settling velocity is verified from solutions of (31) for drop sizes and gas velocities typical of annular flow. For situations with small slip and settling velocities, the theory of Reeks (1977) and experiments by Young & Hanratty (1991) indicate that the drop diffusivity is approximately equal to the fluid diffusivity. Lee *et al.* (1989) showed that the ratio of the root-mean-square of the velocity fluctuations of the particle and the fluid can be approximated as

$$\frac{(\overline{v_y^2})^{1/2}}{(\overline{u_y^2})^{1/2}} = \left(\frac{\beta\tau_f}{0.7+\beta\tau_f}\right)^{1/2}, \qquad [34]$$

where β is the reciprocal time constant of the drop.

For typical conditions in annular flows, the Sauter mean droplet diameter is characterized by $\beta\tau_f \cong 0.01$ to 0.1. From [34] it is seen that $(\overline{v_y^2})^{1/2}/u_* \cong 0.12$ to 0.35, so that droplets are not following the turbulence very well. Furthermore, since $\varepsilon_P = \varepsilon_f$ it follows that

$$\frac{\tau_P}{\tau_f} \cong \frac{0.7+\beta\tau_f}{\beta\tau_f}. \qquad [35]$$

As a consequence, $\tau_P/\tau_f \cong 8$ to 71 for annular flows. The droplet turbulence time scale is much larger than the fluid time scale. This means that it could take a long time to reach a fully developed state and that $f(t-t')$, defined by [13], could increase slowly from its zero value (at $t = t'$) with increasing time.

The above scaling indicates that two dimensionless groups are controlling, $\beta\tau_f$ and Fr. From [18] the turbulent deposition rate to the bottom wall is

$$R_0^T = (\overline{v_y^2})^{1/2}\sqrt{\frac{2}{\pi}} f C_S, \qquad [36]$$

where C_S is the droplet concentration at the surface. Therefore,

$$\frac{k_0^T}{u_*} \propto \frac{(\overline{v_y^2})^{1/2}}{u_*} \frac{C_S}{C_B} f. \quad [37]$$

If C_S/C_B is approximately constant and $f \cong 1/2$, then it would be expected that

$$\frac{k^T}{u_*} \sim \frac{(\overline{v_y^2})^{1/2}}{u_*} = f(\beta\tau_f). \quad [38]$$

This estimate could be valid for conditions under which turbulent deposition dominates and for which the behavior is similar to vertical gas–liquid annular flow. [See, for example, the paper by Binder & Hanratty (1991)].

The contribution of settling to deposition on the bottom wall is given as

$$R_0^S = -V_y(y=0)C_S, \quad [39]$$

where V_y $(y=0)$ is the deterministic velocity of the particles at the bottom boundary. Therefore,

$$\frac{k_0^S}{u_*} = -\frac{V_T}{u_*} \frac{V_y(y=0)}{V_T} \frac{C_S}{C_B}; \quad [40]$$

V_T is the terminal free-fall velocity of the particle. For Stokesian particles

$$\mathrm{Fr}\beta\tau_f = \frac{0.046u_*}{V_T}, \quad [41]$$

so that

$$\frac{k_0^S}{u_*} \propto \frac{1}{\mathrm{Fr}\beta\tau_f} \frac{V(y=0)}{V_T} \frac{C_S}{C_B}. \quad [42]$$

In the limit where gravitational settling is controlling the particles are highly stratified so V_y/V_T and C_S/C_B can be quite different from unity. Since the shapes of the concentration profiles seem to depend primarily on $\beta\tau_f$, an attractive assumption is that

$$\frac{k_0^S}{u_*} \mathrm{Fr}\beta\tau_f = f(\beta\tau_f). \quad [43]$$

5. SOLUTION METHOD

The behavior of a single source is obtained by solving [30] using boundary conditions [11] and [12] made dimensionless by using u_* and H. An explicit finite difference method is used. The diffusion term is represented by a central difference approximation. A forward difference approximation is used for the convective term. The spatial grid is divided into steps h_y and the time step is denoted by h_t. The time, t, is given by

$$t = jh_t, \quad 1 \leqslant j \leqslant J. \quad [44]$$

The channel position, y, is given by

$$y = (i-1)h_y, \quad 1 \leqslant i \leqslant I+1. \quad [45]$$

The concentration at time step $j+1$ is calculated from the concentration at step j by the following equation:

$$C_{i,j+1} = (1 - 2\varepsilon_{P,j}r + V_{y,j}q)C_{i,j} + (\varepsilon_{P,j}r - V_{y,j}q)C_{i+1,j} + \varepsilon_{P,j}rC_{i-1,j} + \mathrm{SOURCE}. \quad [46]$$

Here r and q are defined as

$$r = \frac{h_t}{h_y^2}; \quad q = \frac{h_t}{h_y}. \quad [47]$$

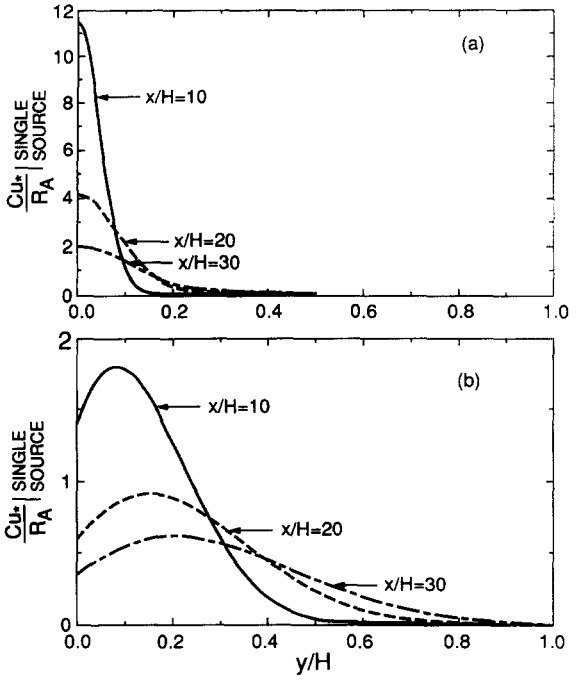

Figure 2. Concentration profiles resulting from an instantaneous source on the bottom wall: (a) Fr = 10, $\beta\tau_f = 0.01$, Re = 100,000; (b) Fr = 10, $\beta\tau_f = 1.0$, Re = 100,000.

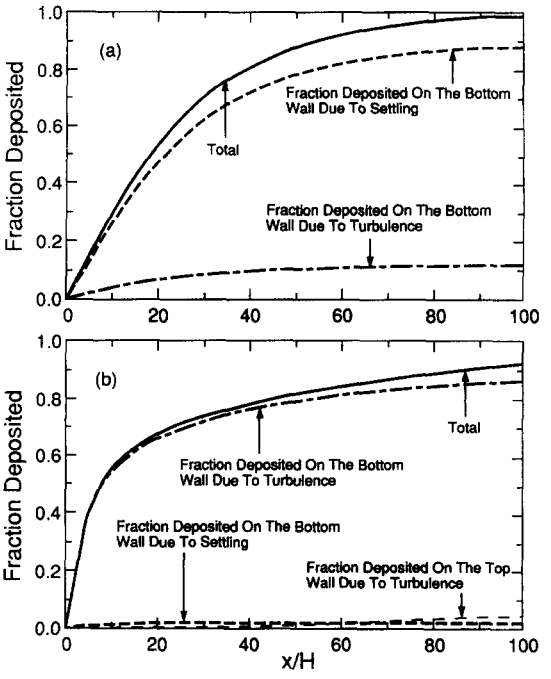

Figure 3. Fraction of the mass from a source on the bottom wall that is deposited: (a) Fr = 10, $\beta\tau_f = 0.01$, Re = 100,000: (b) Fr = 10, $\beta\tau_f = 1.0$, Re = 100,000.

A source on the bottom wall is turned on at $i = 1$ and $j = 0$ and is given by

$$\text{SOURCE} = \begin{cases} \dfrac{Q}{h_y} & \text{for} \quad i = 1 \quad \text{and} \quad j = 0 \\ 0 & \text{for} \quad i \neq 1 \quad \text{and} \quad j \neq 0 \end{cases} \qquad [48]$$

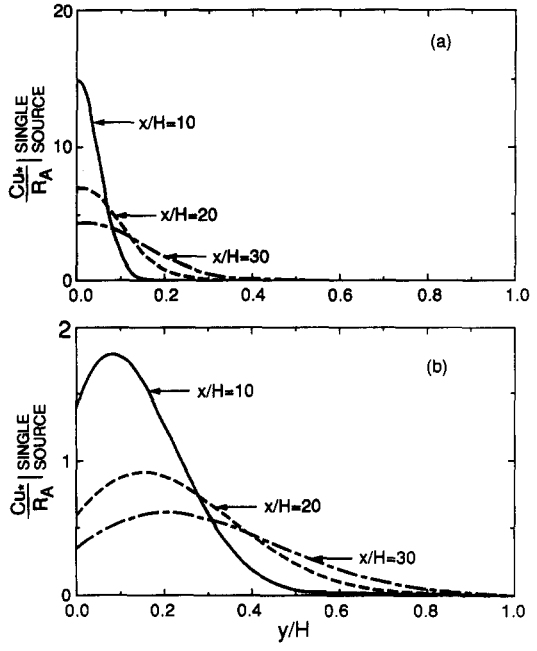

Figure 4. Concentration profiles downstream of an instantaneous source on the bottom wall: (a) Fr = 100, $\beta\tau_f = 0.01$, Re = 100,000; (b) Fr = 100, $\beta\tau_f = 1.0$, Re = 100,000.

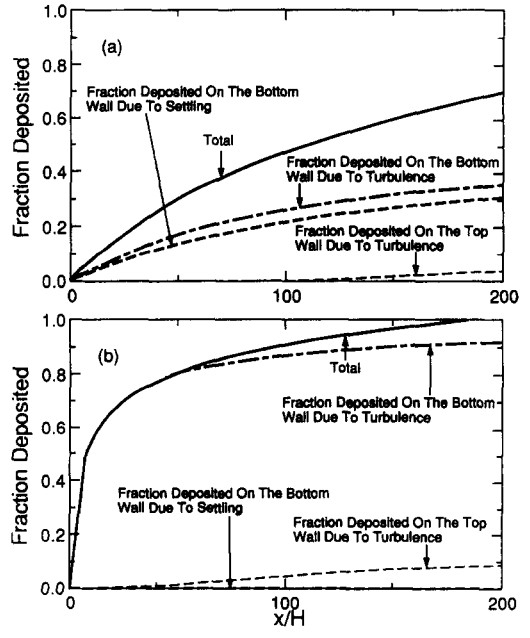

Figure 5. Fraction of the mass originating from a source on the bottom wall that is deposited: (a) Fr = 10, $\beta\tau_f = 0.01$, Re = 100,000; (b) Fr = 100, $\beta\tau_f = 1.0$, Re = 100,000.

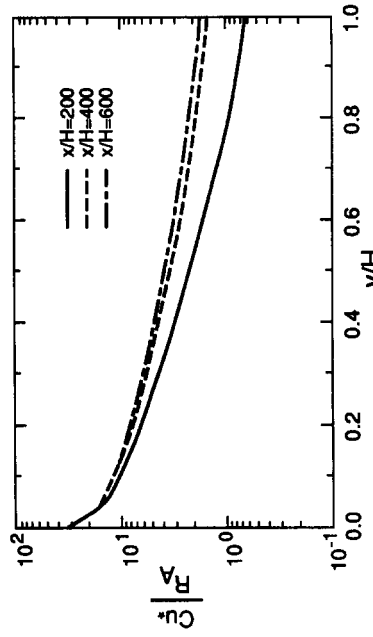

Figure 7. Effect of the length of the flow section on the exit concentration profile for sources on the bottom wall.

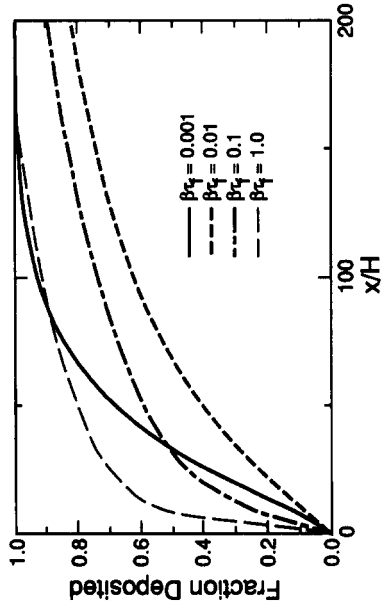

Figure 6. Fraction of the mass from a source on the bottom wall that is deposited; Fr = 50, Re = 100,000.

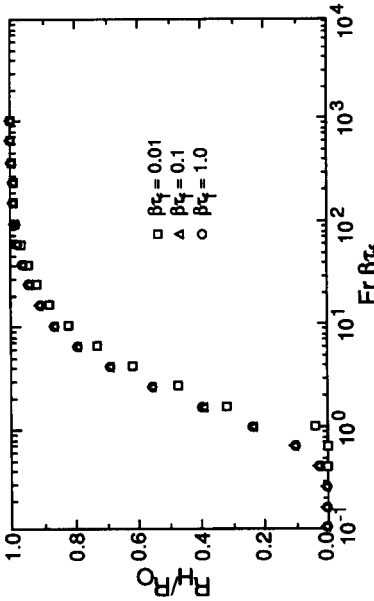

Figure 9. Relative rates of atomization for fully developed flow as a function of Fr $\beta\tau_f$.

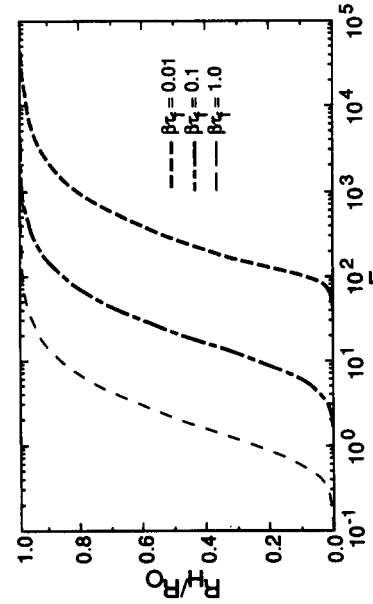

Figure 8. Relative rates of deposition for fully developed flows as a function of Fr.

This has the effect of distributing the source evenly over the first grid point of size h_y. Sources at other locations are represented in an analogous way. The boundary conditions are differenced and are used for writing the difference equations at $i = 1$ and $i = I + 1$. Velocity $V_{y,j}$ is calculated at each time step by a fourth-order Runge–Kutta method. The accuracy of the solution was tested by increasing the number of grid points and choosing q such that the solutions were stable and unchanging. Values of $m = 100$ and $q = 0.01$ were found to be sufficient.

Once solutions for a single source are obtained, a particular concentration field at a given time is calculated by summing over many sources in the following manner:

$$C(y, t) = \int_0^t \left(C(y, t - t') \,\middle|\, \begin{matrix} \text{SINGLE} \\ \text{SOURCE} \end{matrix} \right) \mathrm{d}t'. \qquad [49]$$

This can be used to obtain $C(y, x)$ by substituting $t = x/V_x$, where V_x is the average velocity of the drop in the x-direction.

If the source were of infinitesimal thickness the integral [49] diverges because of a singularity at $t = t'$ (Hanratty 1956). Actually, the source has a finite size, at least equal to the droplet diameter. This has the effect of giving the initial mean-square displacement of the particle a finite value. The computational procedure outlined in [44]–[47] is such that the source thickness equals h_y. For the calculations in this paper $h_y/H = 0.01$. For the range of conditions considered the source thickness, in terms of wall units, is obtained as $10 < h_y u_* / \nu_f < 40$.

6. BEHAVIOR OF A SINGLE SOURCE

The behavior of one instantaneous source, placed on the bottom wall, is interpreted by calculating concentration profiles and the fraction of mass depositing downstream from the source. Results are presented for Fr values from 1 to 100 and droplet inertial parameters from 0.001 to 10.0. The gas phase Re does not enter into the problem directly, other than in converting from time to distance travelled in the streamwise direction. The calculations shown here are for Re = 100,000. The fractions deposited on the lower boundary due to the turbulence or gravitational settling are given separately. The fraction deposited on the top wall due to turbulence is shown, if it occurs.

Figures 2 and 3 give concentration profiles and the fraction deposited for values of Fr = 10 and for $\beta\tau_{LF} (= 1.0, 0.01)$ that are characteristic of large and small drops in annular flows. The profiles shown in figure 2(b) are similar to what was calculated for vertical flows by Binder & Hanratty (1991). At $(t - t') \to 0$ (or $x/H \to 0$) the droplets are primarily moving away from the wall so that $f(t - t') = 0$ in boundary condition [11]. As a consequence, $\partial C/\partial y \cong 0$ and the maximum occurs at $y = 0$. For larger $(t - t')$ or (x/H), where droplets entrained in the turbulence are moving toward the wall, the maximum in the profile moves away from the wall and the positive concentration gradient close to the wall corresponds to the deposition of droplets by turbulence. The concentration profiles in figure 2(a) are for small $\beta\tau_f$, for which $\tau_P/\tau_f = 71$ and $(\overline{v_y^2})^{1/2}/u_* 0.12$. From [13] it is seen that $f(t - t')$ will be approximately zero for a much larger range of times than for the case considered in figure 2(b). As a consequence, the maxima in the droplet concentration profiles are very close to the wall.

Calculations of the fractions deposited, shown in figure 3, are consistent with the concentration profiles. Figure 3(b) shows for $\beta\tau_{LF} = 1.0$ (the small drops) that almost all of the deposition is associated with turbulent transport. It is also noted that at $x/H > 50$ the droplets spread over the whole channel cross section and that some deposition occurs on the top wall. This deposition leads to the buildup of a liquid layer on the top wall which is eventually thick enough that atomization can occur. Figure 3(a) shows just the opposite behavior for the large drops ($\beta\tau_f = 0.01$). Almost all of the deposition occurs by gravitational settling and no deposition occurs by turbulence.

Figures 4 and 5 show the effect of increasing Fr or decreasing the effect of the gravitational field. A comparison of figures 4(b), 5(b) and 2(b), 3(b) indicates that the increase in Fr for $\beta\tau_f = 1.0$ reduces the gravitational deposition to zero but does not have a dramatic effect on the concentration profiles. It is noted that for the cases considered in figure 5 deposition occurs on the top wall.

The conclusion is that the characteristics of the concentration profiles are largely dependent on the value of $\beta\tau_f$. An increase in $\beta\tau_f$ or in Fr increases the relative importance of turbulent deposition over gravitational settling. For large enough Fr the gravitational settling becomes unimportant so deposition is mainly dependent on $\beta\tau_f$.

Figure 6 gives the total fraction of mass deposited from a single source; the effect of the drop size parameter, $\beta\tau_f$, is clearly indicated. Large droplets settle out rapidly because of gravity. Conversely, small drops deposit out quickly due to strong interactions with the gas phase turbulence. Drops with an intermediate size ($\beta\tau_f = 0.01$ for this case) exhibit neither limiting behavior and have longer lifetimes in the gas phase. In annular flows a distribution of droplet sizes is produced by the atomization of the film. The results on the droplet lifetime, shown in figure 5, indicate that the droplet size distribution in the flow field will differ from the distribution at the source. This aging of the droplet distribution is discussed further in the next section.

The results on the behavior of single sources indicate that for certain initial conditions a very long test section is needed to obtain fully developed horizontal annular flow, where the deposition rate equals the atomization rate and the droplet concentration profile is no longer changing downstream. This is demonstrated in figure 7, where droplet concentration profiles are presented for different value of x/H. These were calculated by summing over many single sources, located on the bottom wall, as outlined in section 5. These results are for an Fr (= 50), Re (= 100,000) and droplet size ($\beta\tau_f = 0.01$) representative of air–water annular flows studied in the laboratory. They show that test sections in excess of 600 channel heights may be needed to obtain fully developed annular flow. This calculation disregards the presence of any sources on the top wall. In many situations an atomizing film will also be present on the top wall. Because of the time to build up this film, an even longer test section would be needed to reach a fully developed condition.

7. CONCENTRATION PROFILES FOR FULLY DEVELOPED ANNULAR FLOW

One of the most useful results obtained in the analysis is the prediction of the dimensionless deposition constant, k/u_*, as a function of $\beta\tau_f$ and Fr for fully developed gas–liquid annular flows. Before deposition constants can be calculated the distribution of liquid film flow between the top and bottom wall must be considered. In the experiments of McCoy & Hanratty (1975) and of Namie & Ueda (1972) annular flow was obtained by introducing a liquid film on the bottom wall. This film atomized into droplets; these, in turn, deposited on both walls. A liquid film on the top wall forms and increases in flow rate until it is large enough to atomize. As a consequence, sources on both the bottom and top walls need to be considered to calculate a fully developed droplet concentration profile.

As indicated in the previous section the distance required in these experiments for an atomizing liquid film to form on the top wall may be quite large. McCoy & Hanratty (1975) removed and separately measured the film flow rate for the top and bottom wall at the end of a developing section equal to 260 channel heights in length. They found the liquid film flow rate on the top wall to be an order of magnitude less than on the bottom wall. This is consistent with the findings in the previous section on the fraction of liquid depositing on the top wall. In the experiments of Namie & Ueda the films at the top and bottom walls were withdrawn 250 channel heights downstream of the entrance section. These liquids were combined and then measured.

The effect of gravity on horizontal annular flow can be characterized by considering the relative strengths of sources on the top and bottom walls for fully developed flow. The source strength at the top wall, as compared to the source strength at the bottom wall, can be calculated from a mass balance. For fully developed flow the deposition and atomization rates at each wall must be equal:

$$R_{AH} = R_H \qquad [50]$$

and

$$R_{A0} = R_0 \qquad [51]$$

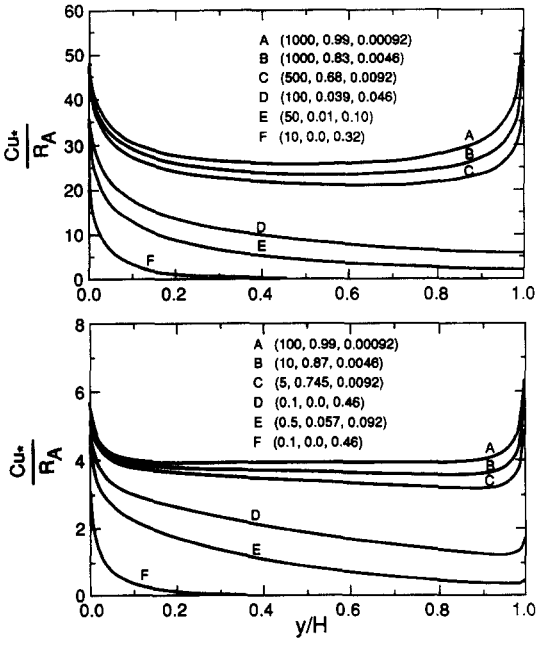

Figure 10. Fully developed concentration profiles in horizontal annular flow. The numbers in parentheses represent (Fr, R_{AH}/R_{A0}, V_T/u_*): (a) $\beta\tau_f = 0.01$; (b) $\beta\tau_f = 1.0$.

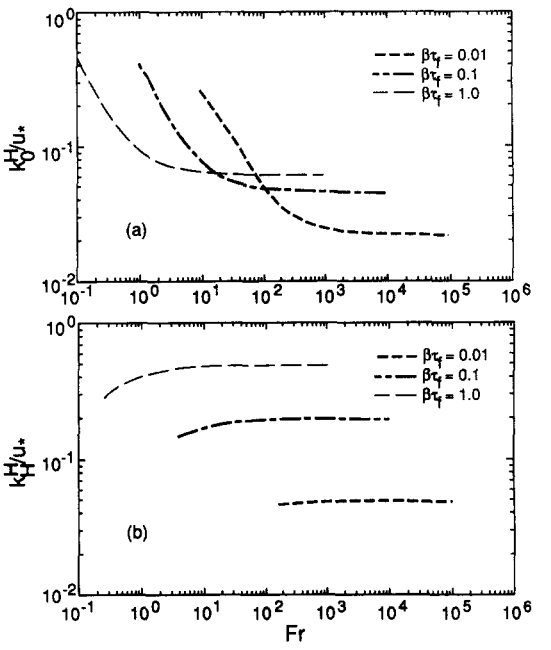

Figure 11. Deposition constants for sources on the bottom wall: (a) k_0^0 represents deposition to the bottom wall; (b) k_H^0 represents deposition to the top wall.

Denote F_{H0} as the fraction of mass entrained at the top wall that deposits on the bottom wall and F_{0T} as the fraction of mass entrained at the bottom wall that deposits on the top. Equations [50] and [51] can be rewritten as

$$R_H = (1 - F_{H0})R_H + F_{0H}R_0 \qquad [52]$$

and

$$R_0 = F_{H0}R_H + (1 - F_{0H})R_0. \qquad [53]$$

By taking the ratio [52]/[53] the following result is obtained:

$$\frac{R_H}{R_0} = \frac{(1 - F_{H0})\dfrac{R_H}{R_0} + F_{0H}}{F_{H0}\dfrac{R_H}{R_0} + (1 - F_{0H})}. \qquad [54]$$

This equation has one physically realistic root,

$$\frac{R_H}{R_0} = \frac{F_{0H}}{F_{H0}}. \qquad [55]$$

Thus, calculations of the fraction deposited for sources placed on the top and bottom wall give the relative rates of deposition for a fully developed flow.

Figure 8 gives the results of a calculation of R_H/R_0 vs Fr for various $\beta\tau_f$ for $x/H = 1000$. It is noted that stratification increases with decreasing Fr or increasing $\beta\tau_f$. Figure 9 plots R_H/R_0 vs the product of Fr and $\beta\tau_f$ which, from [40], is proportional to the reciprocal of V_T/u_*. It is noted that the results for different $\beta\tau_f$ approximately collapse on a single curve.

Figure 9 may be interpreted as a flow regime map for horizontal annular flow. For Fr $\beta\tau_f <$ (0.5 to 0.7), deposition of droplets on the top wall is extremely small. This would seem to correspond to the stratified–annular flow defined by Williams (1990). For (0.5 to 0.7) < Fr $\beta\tau_f <$ (7 to 9) an asymmetric annular flow exists in which the film is unequally distributed on the walls and the droplets are stratified. For Fr $\beta\tau_f >$ (7 to 9) gravitational settling is relatively unimportant and the liquid is distributed symmetrically.

Fully developed droplet concentration profiles, calculated for $\beta\tau_f = 0.01$ and 1.0 are shown in figure 10. These correspond to values of $0.1 < \mathrm{Fr}\,\beta\tau_f < 100$, or $0.00046 < V_T/u_* < 0.32$. The curves for $\mathrm{Fr}\,\beta\tau_f = 0.1$ and 0.5 represent a stratified–annular flow; the curves for $\mathrm{Fr}\,\beta\tau_f = 1.0$ and 5.0, an asymmetric annular flow; the curves for $\mathrm{Fr}\,\beta\tau_f = 10.0$ and 100, a symmetric annular flow.

An understanding of these results can be obtained by considering the distributions downstream of a line source shown in figures 2(a) and 4(a). The curves in figure 10 for $\mathrm{Fr}\,\beta\tau_f = 0.1$ and 1.0 are obtained by summing contributions from all the sources upstream of the location representing that profile. For example, the curves for $x/H = 10$, 20, 30 in figures 2(a) and 4(a) would represent contributions from line sources at locations $x/H = 10$, 20, 30 upstream. The maximum at the wall in the fully developed concentration profiles for $\mathrm{Fr}\,\beta\tau_f = 0.1$ and 1.0 reflects the large contributions of the line sources to the concentration profiles close to the wall, particularly from those at very small x/H. The positive concentration gradients in the line source profiles right at the wall, associated with turbulent deposition, are not seen after averaging over all sources.

The large gradients at $y/H = 1$, shown in figure 10, reflect the existence of sources of drops at the top wall. For $\mathrm{Fr}\,\beta\tau_f = 0.1$ and 0.5 gravitational effects are large enough for negligible atomization to occur at the top wall. For large $\mathrm{Fr}\,\beta\tau_f$ the strengths of the sources on the top wall are large enough that the behaviors of the concentration profiles are the same at both walls.

8. DEPOSITION RATES FOR FULLY DEVELOPED ANNULAR FLOWS

Figures 11 and 12 present deposition constants for cases in which sources exist only at the bottom or at the top wall. These results may be thought of as representing a (fictitious) situation in which liquid reaching the top (or bottom) wall is removed and returned to the bottom (or top) wall. Constants characterizing the deposition rates to the bottom and top walls are defined as

$$k_0^i = \frac{R_0}{C_B^i} \qquad [56a]$$

and

$$k_H^i = \frac{R_H}{C_B^i}, \qquad [56b]$$

where superscript i signifies where the sources are located and C_B^i is the bulk concentration calculated for sources on the ith wall. At Fr large enough that $\mathrm{Fr}\,\beta\tau_f > 20$, it is seen, in agreement with [38], that k_0^i/u_* depends only on $\beta\tau_f$. At low Fr, figures 11(a) and 12(a) show that k_0^i/u_* varies approximately as Fr^{-1}, in agreement with [43]. Furthermore, it should be noted that the labels on the ordinate in figure 11(b) are much smaller than those in figure 11. This reflects the much lower rates of deposition on the top wall than on the bottom wall.

The results presented in figures 8, 11 and 12 can be used to calculate deposition constants for fully developed annular flow. The bulk concentration for sources at both the top and bottom walls is calculated as

$$C_B = C_B^H + C_B^0. \qquad [57]$$

These concentrations are related to the deposition constants in figures 11 and 12 as follows:

$$C_B^0 = \frac{R_0}{k_0^0 + k_H^0} \qquad [58]$$

and

$$C_B^H = \frac{R_H}{k_0^H + k_H^H}. \qquad [59]$$

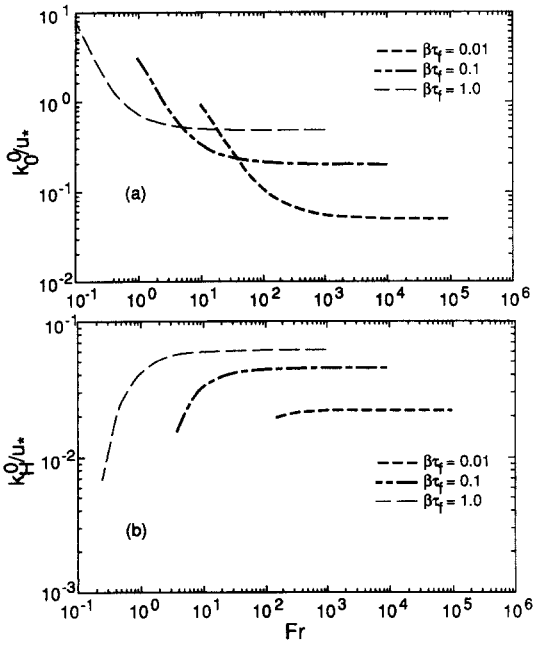

Figure 12. Deposition constants for sources on the top wall; (a) k_0^H represents deposition to the bottom wall; (b) k_H^H represents deposition to the top wall.

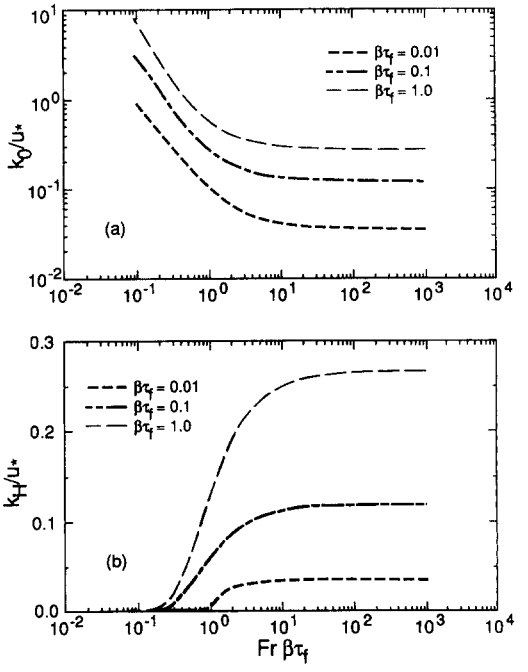

Figure 13. Deposition constants for fully developed annular flow, i.e. for sources on the top and bottom walls: (a) k_0 represents deposition to the bottom wall; (b) k_H represents deposition to the top wall.

A fully developed deposition constant for the bottom wall, $k_0 = R_0/C_B$, is calculated as follows by using [57]–[59] to calculate C_B:

$$k_0 = \frac{1}{\dfrac{1}{k_0^0 + k_H^0} + \dfrac{R_H}{R_0}\dfrac{1}{k_0^H + k_H^H}}. \qquad [60]$$

The deposition, constant for the upper wall, $k_H = R_B/C_B$, is related to k_0 as follows:

$$k_H = \frac{R_H}{R_0} k_0. \qquad [61]$$

Figure 13 presents deposition constants for fully developed flow. It is noted that for Fr $\beta\tau_f > 20$ the deposition constants for the top and bottom walls, depend only on $\beta\tau_f$ and are approximately equal (see [38]). For Fr $\beta\tau_f < 20$, the settling velocity becomes important and the deposition constants for the top wall become significantly less than those for the bottom wall. At Fr $\beta\tau_f < 0.2$ gravitational settling dominates, deposition to the top wall is negligible and the deposition constant varies with $(\text{Fr}\,\beta\tau_f)^{-1}$ for fixed $\beta\tau_f$ (see [43]).

Equation [37] suggests for large Fr $\beta\tau_f$ that k should vary approximately with $(\overline{v_y^2})^{1/2}$. Therefore, the deposition constant representing the total deposition,

$$k = k_0 + k_H, \qquad [62]$$

is plotted in figure 14 as $k/(\overline{v_y^2})^{1/2}$ vs Fr $\beta\tau_f$. The values of $(\overline{v_y^2})^{1/2}$ are obtained from [34]. It is noted that in this type of plot the influence of $\beta\tau_f$ becomes small.

9. COMPARISON WITH LABORATORY MEASUREMENTS

The conditions for the experiments of McCoy & Hanratty (1975) and Namie & Ueda (1972) are summarized in table 1. Drop sizes, obtained from a correlation by Azzopardi (1985) for vertical annular flow, are used because reliable measurements for horizontal flows are not available over a wide enough range of conditions. It is believed that this correlation would be satisfactory if

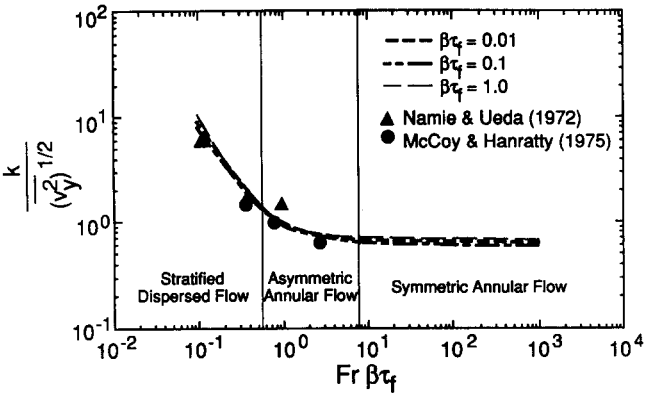

Figure 14. Comparison of calculated total deposition rates with measurements, $k = k_0 + k_H$.

gravity is not influencing the atomization process. Differences in the measurements of k/u_*, which had been puzzling, can now be interpreted.

The experiments of Namie & Ueda (1972) were carried out in a smaller channel and for larger Fr. Both studies were carried out for a range of Fr $\beta\tau_f$ that would indicate that gravitational settling was having a strong effect on the concentration profiles. This is illustrated in figure 14, where the data of McCoy & Hanratty (1975) and of Namie & Ueda (1972) have been plotted.

Reasonably good agreement is found between the calculations and the data. However, it should be noted that the data were obtained for somewhat different conditions than were used in the calculations. In the experiments, the film was removed from the wall and deposition rates were measured downstream of an approximately fully developed condition. It is, therefore, of interest to calculate deposition constants downstream of a location where the source is turned off. Experiments in vertical annular flow (Cousins & Hewitt 1968) indicate that deposition constants decrease downstream of the film removal section. Binder & Hanratty (1991) showed that this could be due to a change in the shape of the concentration profile. In horizontal annular flow the effect of the deposition length is more complicated.

Figure 15 shows calculated deposition constants for the bottom and top walls at various locations downstream, after turning off the sources. For this calculation the sources were located only at the bottom wall. The deposition constants are plotted vs $\beta\tau_f$ in order to exhibit the differing behavior of small and large droplets. Figure 16 presents the concentration profiles, after turning off the source, for two different $\beta\tau_f$. Figures 15 and 16 were calculated for Fr = 10. The two values of $\beta\tau_f = (0.01$ and $1.0)$, used in figure 15, exhibit the limiting behavior of very large and very small particles.

For large $\beta\tau_f$ (small particles) deposition constants show the same results as is found for vertical flow; ie. they decrease with increasing distance downstream. The deposition rate is controlled by turbulent diffusion and is affected by changes in the concentration profiles, shown in figure 16(b). The shape of the concentration profile and, therefore, the deposition rate remains the same at the top wall. However, the bulk concentration decreases, so the deposition constant for the top boundary increases.

Table 1. Conditions of the experiments by McCoy & Hanratty (1975) by Namie & Ueda (1972)

Fr	$d_{32}(\mu m)$	$\beta\tau_f$	k/u_*
Namie & Ueda (1972), H = 0.01 m			
33.4	86	0.011	0.056
50.4	66	0.016	0.046
98.4	42	0.027	0.039
McCoy & Hanratty (1975), H = 0.0254 m			
5.67	130	0.019	0.30
11.5	81	0.034	0.12
19.0	58	0.052	0.13

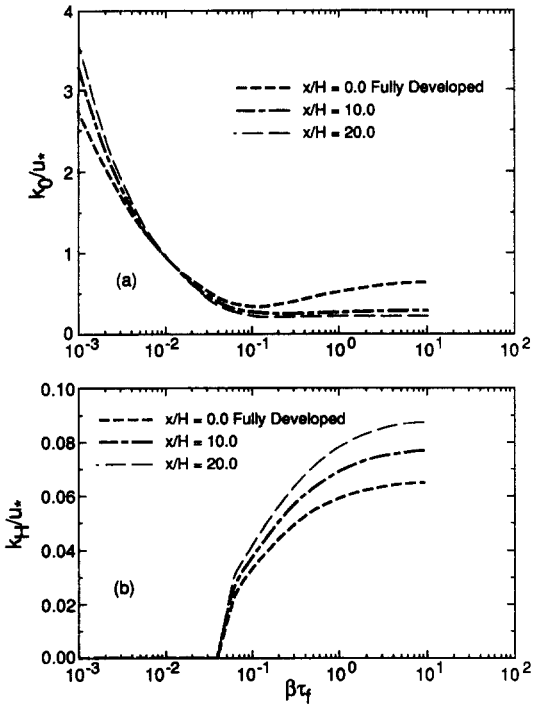

Figure 15. Deposition constants in horizontal annular flow downstream of a film removal station for Fr = 10: (a) k_0 is the deposition constant for the bottom wall; (b) k_H is the deposition constant for the top wall.

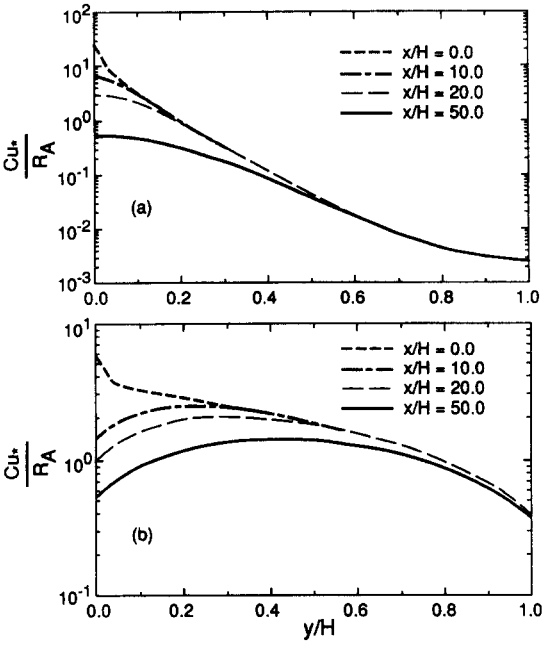

Figure 16. Concentration profiles downstream of a film removal station for Fr = 10: (a) $\beta\tau_f = 0.01$; (b) $\beta\tau_f = 1.0$.

For small $\beta\tau_f$ (large particles) there is no deposition on the top wall and the deposition constant to the lower boundary increases downstream of the film removal section. Here the deposition is controlled by gravitational settling; this is evidenced by the small concentration gradient at $y = 0$, shown in figure 16(a). The increase in the deposition constant is due to an increase in the average settling velocity of the droplets to the terminal value. This occurs downstream of the film removal section because no new sources of droplets are entering the channel.

It is, therefore, found that the measured deposition constants may increase or decrease downstream of a suckoff unit, depending on the controlling process for the deposition. Calculations for the conditions characterizing the experiments indicate that the deposition constant would stay approximately constant for the mean drop size. In actual annular flow there is a distribution of droplet sizes. At the present time incomplete information is available on the atomization process, so a more complete analysis of the experiments cannot be done. It is tentatively concluded that

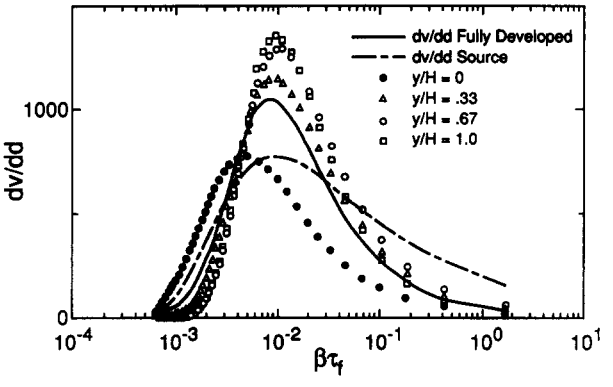

Figure 17. Comparison of droplet size distribution in horizontal annular flow with the size distribution originating from the source.

the deposition constants measured by McCoy & Hanratty (1975) and by Namie & Ueda (1972) are approximately equal to the fully developed values.

10. DROP SIZES

Despite the fact that little experimental data are available, the present analysis can be used to provide some insight into phenomena affecting the droplet size distribution in annular flow. In order to discuss these phenomena a drop size distribution function of the source is assumed. A convenient choice is the Rossin–Rammler function, defined as

$$1 - v = \exp\left[-\left(\frac{d}{d_R}\right)^{\Delta}\right], \qquad [63]$$

where $1 - v$ is the volume fraction of the droplets emitted by the source with diameter greater than d. Azzopardi (1978) fitted measurements of droplet size in vertical annular flow to [63]. Examination of these data suggests reasonable choices for Δ and d_R. For all flow conditions Δ ($\cong 1.8$) was approximately constant. By plotting d_R vs the Sauter mean diameter, given by the correlation of Azzopardi (1985), a linear relation was determined. By dividing the droplet distribution into N increments of size Δd the droplet concentration is calculated from

$$C(y, t) = \sum_{i=1}^{N} \left(\frac{\mathrm{d}v}{\mathrm{d}d}\right)_i C_i(y, t)\, \Delta d, \qquad [64]$$

where C_i is the solution of the mass balance equation for the ith size.

Figure 17 shows droplet distribution functions vs $\beta\tau_f$ for sources on the lower wall. The figure compares the distribution in the source, given by [64], to the distribution for all of the droplets in the gas under fully developed conditions. It is clear that the fully developed droplet distribution narrows, with the peak tending to the droplet with the longest lifetime or the smallest deposition constant. The droplet size distributions at different y/H indicate, as expected, that the larger particles remain in the lower portion of the pipe.

11. CONCLUDING REMARKS

A Lagrangian approach has been explored to describe the distribution and deposition of drops in horizontal turbulent flows. The principal idea is to describe the concentration field as resulting from distributions of approximately infinitesimal sources. The problem is simplified by assuming that the turbulence is homogeneous and that the mean velocity field of the fluid is uniform. This, then, limits the application of the results to particles characterized by large enough $1/\beta^+$ (>20) that their stopping distances are greater than the thickness of the viscous wall region.

Point source behavior is described by Taylor's theory so that the influence of the time dependency of the diffusion process is taken into account. This, in effect, causes diffusion coefficients close to the wall to be smaller since drops in this region have, on average, been in the field for shorter times.

The influence of gravity on the drop distributions is calculated by assuming that the gravitational field acts independently of the turbulence to give a deterministic average trajectory for the particles. A weakness of this calculation is that not enough is known about how the particles enter the field. In order to implement the analysis it is assumed that, on average, the initial velocity in the y-direction is proportional to the root-mean square of the turbulent velocity fluctuations of fully entrained drops and that the initial velocity in the x-direction is the same as the gas.

Drops are assumed to be permanently removed from the field when they impact on a boundary. For molecular diffusion, a completely absorbing boundary, such as this, would dictate that the concentration be zero at the boundary. However, as pointed out by Lee *et al.* (1989), the large scale characterizing the random motion of drops requires a finite concentration which is defined by [11] and [12] for a single source. The actual concentration at the boundary, which is calculated by summing the contributions of all the sources, depends on the strength of the sources.

The analytical framework that has been developed defines the dimensionless groups that control the degree of the stratification of particles and the rate of deposition in horizontal gas–liquid annular flows. They are the ratio of the time scale of the fluid to the time scale of the particles, $\beta\tau_f$, and the Fr $(=u_*^2/gH)$. The product of the two groups decreases with increasing V_T/u_* and it is found that stratification increases with decreasing values of this group. For small Fr $\beta\tau_f$ the deposition rate is controlled by gravitational settling; for large Fr $\beta\tau_f$ it is controlled by the fluid turbulence.

Finally, it should be pointed out that, because of the approximations made in this analysis, exact quantitative agreement with measurements cannot be made. Of particular importance would be the availability of precise results about how droplets enter the field. Further calculations should explore the sensitivity of the results to the choice of V_y' and V_x', the effects of ignoring the influences of flow non-homogeneities, and errors associated with turbulence effects on C_D when solving [5].

Acknowledgements—This work has been supported by the National Science Foundation under Grant NSF CTS 89-19343 and by the Department of Energy under Grant DOE DEF 602-86er13556.

REFERENCES

ANDERSON, R. J. & RUSSELL, T. W. F. 1970 Film formation in two phase annular flow. *AIChE Jl* **16,** 626–633.

AZZOPARDI, B. J. 1978 Measurement of drop sizes. *Int. J. Heat Mass Transfer* **22,** 1245–1279.

AZZOPARDI, B. J. 1985 Drop sizes in annular two-phase flow. *Expts Fluids* **3,** 53–59.

BINDER, J. L. & HANRATTY, T. J. 1991 A diffusion model for droplet deposition in gas/liquid annular flow. *Int. J. Multiphase Flow* **17,** 1–11.

COUSINS, L. B. & HEWITT, G. F. 1968 Liquid phase mass transfer in annular two-phase flow: droplet deposition and liquid entrainment. UKAEA Report AERE-R5657.

ECKLEMAN, L. D. & HANRATTY, T. J. 1972 Interpretation of measured variations of the eddy conductivity. *Int. J. Heat Mass Transfer* **15,** 2231–2239.

HANRATTY, T. J. 1956 Heat transfer through a homogeneous isotropic turbulent field. *AIChE Jl* **2,** 42–45.

HANRATTY, T. J. 1958 Note on the analogy between momentum transfer and heat or mass transfer for a homogeneous isotropic turbulent field. *AIChE Jl* **1,** 495–496.

HANRATTY, T. J. & FLINT D. L. 1958 Velocity profile for fully developed turbulent flow in a pipe. *AIChE Jl* **4,** 132–136.

JAMES, P. W., WHALLEY, P. B. & HEWITT, G. F. 1980 Droplet motion in two-phase flow. Presented at the *Int. Topic. Mtg. on Nuclear Reactor Thermal Hydraulics*, Saratoga Springs, NY.

LEE, M. M., HANRATTY, T. J. & ADRIAN, R. J. 1989 The interpretation of droplet deposition measurements with a diffusion model. *Int. J. Multiphase Flow* **15,** 459–469.

MCCOY, D. D. & HANRATTY, T. J. 1975 Rate of deposition of droplets in annular two-phase flow. *Int. J. Multiphase Flow* **3,** 319–331.

NAMIE, S. & UEDA, T. 1972 Droplet transfer in two-phase annular mist flow. *Bull. JSME* **15,** 1568–1580.

PISMEN, L. M. & NIR, A. 1978 On the motion of suspended particles in stationary turbulence. *J. Fluid Mech.* **84,** 193–206.

REEKS, M. W. 1977 On the dispersion of small particles suspended in an isotropic turbulent fluid. *J. Fluid Mech.* **83,** 529–546.

TAYLOR, G. I. 1921 Diffusion by continuous movements. *Proc. Lond. Math. Soc.* **151,** 196–211.

VAMES, J. S. & HANRATTY, T. J. 1988 Turbulent dispersion of droplets for air flow in a pipe. *Expts Fluids* **6,** 94–104.

WILLIAMS, L. R. 1990 Effect of pipe diameter on horizontal annular flows. Ph.D. Thesis, Univ. of Illinois, Urbana, IL.

YOUNG, J. B. & HANRATTY, T. J. 1991 Optical studies of the turbulent motion of solid particles in a pipeflow. *J. Fluid Mech.* **231,** 665–688.